A 3D-Fourier-Descriptor Approach to Compress 3D Imaging Data

Robert Schmitt and Peter Fritz
Laboratory for Machine Tools and Production Engineering (WZL), RWTH Aachen University
Steinbachstraße 19, Aachen, 52074, Germany

Introduction

One major problem of optical 3D measurement methods like structured light projection or computer tomography is the size of the resulting scans. For example, a medium-sized CT data set with a resolution of 1000 × 1000 × 1000 voxels and a standard bit depth per voxel of 16 Bit takes 1.9 GB. Hence, much effort has to be spent to carry out the measurement, to archive the data, or to transmit the scans to other manufacturing units. A remedy for this problem is the compression of the recorded point clouds. In contrast to previous research work, where we proposed a method for lossless compression of computer tomography point clouds [1], this paper provides lossy compression techniques to achieve higher compression rates.
Fourier Descriptors are introduced in [2], to provide a compact representation for 2-dimensional shapes. In [3], Kim adopted this method to a lossy compression scheme for 3D-digitized engineering components. The key aspect of this method is to represent a point cloud by a series of periodic base functions. For this, the 3D model is divided into N slices and each point (x_n, y_n) within slice n is considered as complex value. The points on each slice form a continuous 2D-shape contour. This contour is transformed from the geometric domain to the frequency domain by applying the Fast Fourier Transform (FFT). In the frequency domain, the information of the signal is concentrated in very few elements. This implies that the absolute values of most Fourier coefficients are extremely small compared to the signal energy. Setting these coefficients to zero and keeping only values above a certain threshold implies only small changes in the signal and small compression errors. The remaining Fourier coefficients are referred to as *Fourier Descriptors (FD)*. The method yields a distinct compression of the initial 3D shape model—Kim reported compression rates of 88.5 up to 95 percent compared to 55 percent in [1]. The initial 3D shape model can be recovered by retransforming the Fourier descriptors to the geometric domain.

Background

The key aspect of geometrical Fourier analysis is to represent the scanned data by orthogonal basis functions. For the 2-dimensional case, we consider a discrete sequence $f(n)$ that is sampled from a continuous function. The *Discrete Fourier Transform (DFT)* is defined by

$$F(w) = \frac{1}{N}\sum_{n=1}^{N-1} f(n)\cdot \exp(-\mathrm{j}2\pi w\, n/N), \tag{1}$$

with N as number of samples and $w = 0, 1, \ldots, N-1$ are the respective frequencies in the frequency domain. Consider that each 2D point ($x(n)$, $y(n)$) of a given 2D contour can be represented by a complex number $z(n) = x(n) + \mathrm{j}\cdot y(n)$. The complex *Fourier Descriptor (FD)* of the shape is defined by

$$F(w) = \frac{1}{N}\sum_{n=1}^{N-1} (x(n) + \mathrm{j}\, y(n))\cdot \exp(-\mathrm{j}2\pi w\, n/N). \tag{2}$$

For shapes, where each point is a function of the angle φ and r (i.e. there are no re-entrant angles), (2) can be denoted in the polar form as

$$F(w) = \frac{1}{N}\sum_{n=1}^{N-1} (r(\varphi_n)\cdot \exp(\mathrm{j}\varphi_n))\cdot \exp(-\mathrm{j}2\pi w\, n/N). \tag{3}$$

Figure 1 shows an example of this angular parameterization of a shape. If the object is rotated by an a constant angle φ_0, it can be shown that the initial FD $F(w)$ changes to $F'(w) = F(w)\cdot \exp(\mathrm{j}\varphi_0)$. We can eliminate this rotation, by taking the absolute value of the FD and have $|F'(w)| = |F(w)|$. This provides a *rotation-free* representation of the initial object. Applying the modulation theorem [4], we can derive that $F(w-1) = \mathcal{F}\{r(\varphi)\}$, i.e. we can discard the angular factor $\exp(\mathrm{j}\varphi_n)$ of the polar form in (3), because this factor only applies a circular shift of the Fourier coefficients in the Fourier domain. We result in the final equation for rotation-free angular-parameterized FD, which is simply the Fourier transform of the radii:

$$F(w) = \frac{1}{N}\sum_{n=1}^{N-1} r(\varphi_n)\cdot \exp(-\mathrm{j}2\pi w\, n/N) \tag{4}$$

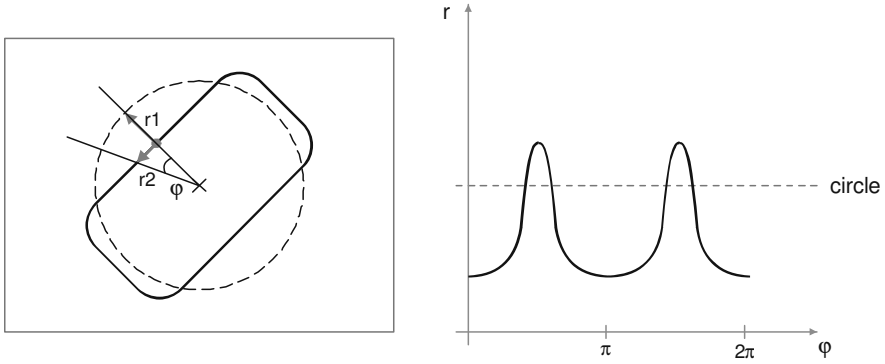

Figure 1: Angle representation of an object.

Proposed Method

In this chapter, we expand the theory of Fourier descriptor to 3 dimensions. In [2], Kim extends the $r = f(\varphi)$-parameterization to $r = f(\varphi/z)$, which are the 3D polar coordinates. The point cloud is separated into several 2-dimensional N slices with thickness dz and each of the slice is treaded as a 2D shape (see Figure 2). We denote this type of FD as *Cylindrical Fourier Descriptor* to distinguish it from 2D-FD and the spherical FD. The cylindrical FD is defined by

$$C1(v,w) = \frac{1}{N}\sum_{n=1}^{N-1} r(\varphi_n, z_v)\cdot \exp(-\mathrm{j}2\pi w\, n/N)\,. \tag{5}$$

To incorporate also interrelations on the z-axis, we introduced a modified cylindrical FD that is computed by a 2D-FFTand is given by

$$C2(v,w) = \frac{1}{M\cdot N}\sum_{m}^{M-1}\sum_{n=1}^{N-1} r(\varphi_m, z_n)\cdot \exp(-\mathrm{j}2\pi\,(vm/M + wn/N))\,. \tag{6}$$

These 2 descriptors are well suited to represent cylindrical objects: For example, consider a regular cylinder with centroid $(0\ 0\ 0)^T$ and radius r = 1. The resulting FD C1 and C2 are given by

$$C1 = \begin{pmatrix} 1 & 0 & \cdots & 0 \\ 1 & 0 & \cdots & 0 \\ \vdots & \vdots & \ddots & 0 \\ 1 & 0 & 0 & 0 \end{pmatrix} \text{ and } C2 = \begin{pmatrix} 1 & 0 & \cdots & 0 \\ 0 & 0 & \cdots & 0 \\ \vdots & \vdots & \ddots & 0 \\ 0 & 0 & 0 & 0 \end{pmatrix}, \tag{7}$$

which is a distinct reduction of redundancy of the shape representation. An obvious method to represent sphere-like objects is the spherical representation i. e. by parameterize the shape by $r = f(\varphi/\vartheta)$. This *Spherical 3D Fourier Descriptors* is denoted by

$$S(v,w) = \frac{1}{M\cdot N}\sum_{m}^{M-1}\sum_{n=1}^{N-1} r(\varphi_m, \theta_n)\cdot \exp(-\mathrm{j}2\pi\,(vm/M + wn/N))\,. \tag{8}$$

As for the C2, we also apply a 2D-FFT on the extracted radii. Figure 2 provides a visualization of both types of 3D-FDs.

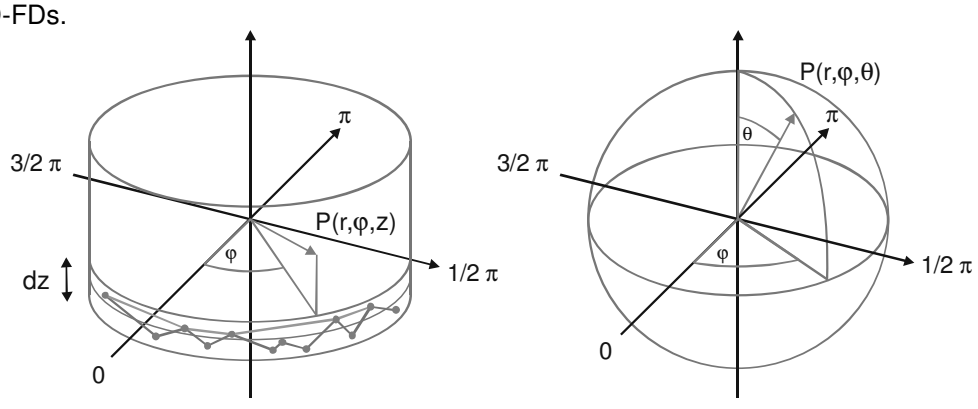

Figure 2: Cylindrical and spherical parameterization.

Experimental Results

To evaluate our method, we used point clouds from 3 different scanned shapes: The first is a spacer, whose surface contains of several connected and intersected regular planes. The second is a bevel gear, which has neither a cylindrical nor a spherical, but a conical shape. Apparently, the surface of the gear has higher frequency elements than the other shapes. The third component is a molding cast. It was selected to evaluate the selected descriptors on free-form elements. We have selected the models from [5]. Due to re-entrant angles, it is not possible to generate cylindrical FDs of the molding cast and hence, only results of the S-FD are available on the last shape.

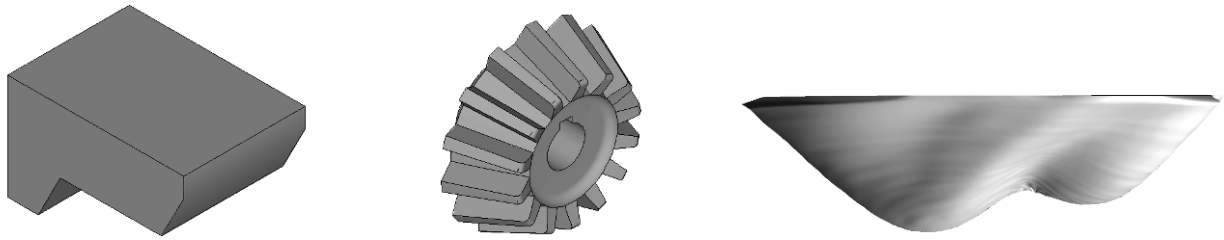

Figure 3: Experimental Data. a) Spacer, b) bevel gear, c) molding cast.

The number of extracted point has been fixed to 6000 to make the results comparable. In the first step, the points are parameterized using the proposed methods of the previous chapter. For the descriptors C1 and C2, the result is a matrix with φ indicating the rows, z the columns, and the radius r are the elements of the matrix. S is organized in the same way with respectively the elevation angle θ as column index.
After applying the Fourier transform of the corresponding descriptor on the data, the magnitude of the higher frequency coefficients are extremely small compared to lower frequencies. If these coefficients are discarded, the original signal (i.e. the point cloud) only changes slightly. Of course, discarding too many frequency coefficients effects in compression artifacts in the point-cloud signal. In this paper, we discarded the high-frequency coefficients by setting the corresponding matrix element to zero. Each frequency element is quantized using 4 Bytes. For an additional compression improvement, we arranged the matrix in a zigzag manner and applied both run length [6] and entropy encoding [7].

Table 1: Experimental Setup

Object	Type	Size x / y / z [mm]	Extracted points	Resolution C-FD [φ / z]	Resolution S-FD [φ / θ]
Spacer	Regular, cuboid	60 x 40 x 35	6000	200 x 30	80 x 75
Bevel Gear	Conical	200 x 200 x 100	6000	200 x 30	80 x 75
Molding cast	Free-form	28 x 39 x 9	6000	200 x 30	80 x 75

Table 2 to Table 8 give the results of the compression experiments. We gradually discarded 0 percent to 99 percent of the extracted Fourier descriptors and reconstructed the point clouds. Even, if any FD coefficient is discarded, we obtained a distinct compression caused by the quantizing operation and the following encoding steps. The peak error can be displayed by the peak-signal-to-noise-ratio (PSNR) that describes the ratio between the maximum possible power of a signal and the power of the compression artifacts. To measure the average error of each scanned point within the point cloud, we evaluate the uncertainty of each measured point by computing the standard deviation. All setups have to be compared on equal compression rates.
The 1D-FFT cylindrical FD C1 outperforms the 2D-FFT C2 at almost all setups. At same compression rates, the standard deviation of C2 is higher than C1. Hence, it is not possible in praxis to increase the compression efficiency of cylindrical FDs by the 2D-FFT approach, although equation (7) assumes this.
Applying the S-FD yields an additional improvement in compression rates. The spherical φ/θ–parameterization suffers less from discard FD coefficiants with lower magnitudes, especially on the bevel-gear shape.

Table 2: Spacer C1

Remaining points [%]	Compression rate [%]	PSNR [dB]	Std. dev. [mm]
100	86.4	129.7	0.0166
90	86.4	129.7	0.0166
75	86.7	128.8	0.0175
50	88.4	122.5	0.0252
25	91.6	105.5	0.0667
10	**95.1**	**82.8**	**0.2467**
5	97.2	70.2	0.5104
1	99.2	43.6	2.3624

Table 3: Spacer C2

Remaining points [%]	Compression rate [%]	PSNR [dB]	Std. dev. [mm]
100	55.8	159.2	0.0030
90	57.2	118.4	0.0318
75	61.7	100.7	0.0884
50	71.4	87.7	0.1869
25	85.0	77.7	0.3318
10	92.4	70.8	0.4936
5	**95.6**	**66.0**	**0.6405**
1	98.7	49.8	1.6643

Table 4: Spacer S

Remaining points [%]	Compression rate [%]	PSNR [dB]	Std. dev. [mm]
100	65.2	203.4	< 0.0001
90	89.2	95.3	0.0300
75	89.2	95.3	0.0300
50	90.0	93.3	0.0340
25	92.3	87.0	0.0490
10	**95.7**	**81.5**	**0.0670**
5	97.3	76.4	0.0900
1	99.1	57.2	0.2730

Table 5: Bevel gear C1

Remaining points [%]	Compression rate [%]	PSNR [dB]	Std. dev. [mm]
100	71.7	151.0	0.0149
90	71.7	151.0	0.0149
75	71.7	151.0	0.0149
50	76.2	114.3	0.1231
25	85.0	94.0	0.3949
10	91.8	79.3	0.9220
5	**95.0**	**66.9**	**1.8852**
1	95.1	46.9	5.9406

Table 6: : Bevel gear C2

Remaining points [%]	Compression rate [%]	PSNR [dB]	Std. dev. [mm]
100	59.2	178.3	0.0031
90	60.3	103.7	0.2256
75	63.8	88.1	0.5537
50	72.2	74.6	1.2078
25	83.6	64.2	2.1938
10	91.7	57.4	3.2445
5	**94.8**	**54.1**	**3.9362**
1	98.3	50.2	4.9037

Table 7: Bevel gear S

Remaining points [%]	Compression rate [%]	PSNR [dB]	Std. dev. [mm]
100	64.2	170.3	0.0038
90	65.1	140.6	0.0207
75	67.8	124.1	0.0539
50	74.9	109.0	0.1282
25	84.5	95.2	0.2843
10	91.2	83.2	0.5668
5	**94.5**	**74.4**	**0.9397**
1	98.1	58.1	2.4142

Table 8 Molding Cast S

Remaining points [%]	Compression Rate [%]	PSNR [dB]	Std. dev. [mm]
100	64.4	144.7	0.0030
90	64.4	144.7	0.0030
75	65.1	141.0	0.0037
50	70.3	130.2	0.0069
25	80.4	118.3	0.0138
10	90.3	108.6	0.0240
5	**94.3**	**94.5**	**0.0544**
1	97.9	64.9	0.2979

When discarding more than 99% of all FD coefficients, the compression artifacts becomes visible for the human eye. Figure 4 provides a graphical survey of different decimation ratios on the spherical FDs of the gear shape. Notice that the more the figure changes to sphere, the more coefficients we discard. If only one single S-FD coefficients is kept (i. e. the DC component of the radii), the result would be a sphere with a radius that is defined by this coefficient.

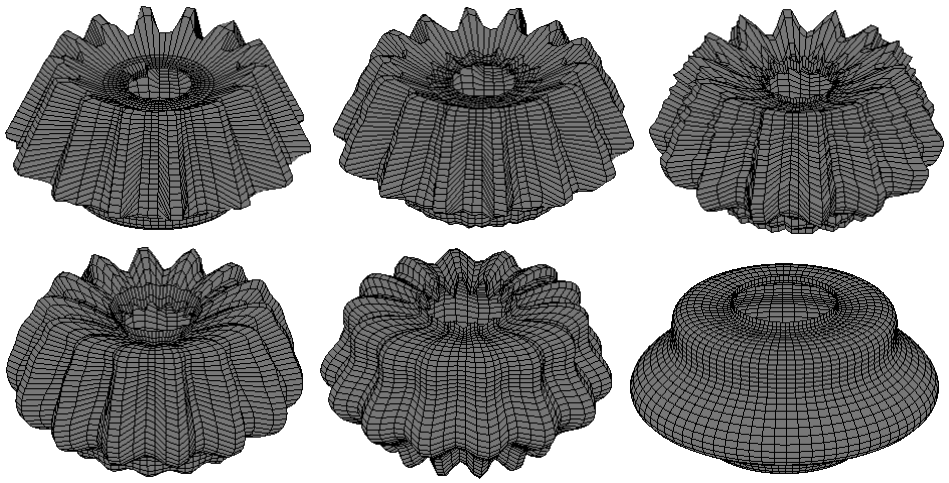

Figure 4: Compression errors by discarding S-FD coefficients. Discarding: a) 0% of the FD-coefficients, b) 97.5%, c) 99%, d) 99.5%, e) 99.75%, f) 99.9%

Conclusion and Outlook

We presented 3 different adaptations of Fourier Descriptors to deal with 3D point clouds. Experiments with 3 scanned objects showed that Fourier-based compression techniques provide a considerable compression of the initial point clouds and cause only moderate compression artifacts. Among all applied descriptors, the S-FD was the best on the all tested shapes. A problem that has still to be solved is how to deal with re-entrant angles. Future research will focus on enhancing the concept of spherical FDs to S*pherical Harmonics*.

Acknowledgments

This work was funded by the Deutsche Forschungsgemeinschaft (DFG) under contract no. SCHM 1856/4-1.

Literature

[1] R. Schmitt and P. Fritz “Lossless Compression of Computer Tomography Point Clouds”, in *IMEKO Conference of Advanced Mathematical and Computational Tools in Metrology and Testing (AMCTM)*, 2008.

[2] C. T. Zahn and R. T. Ralph Roskies, "Fourier Descriptors for Plane Closed Curves", in *IEEE Transactions on Computers*, Vol. c-21, No. 3, pp.269–281, 1972.

[3] H. M. Kim, J. H. Ryu, Y. G. Lee and K. H. Lee, “A new contour data compression method using Fourier descriptor“, in *International Journal of Advanced Manufacturing Technology*, Vol. 28, No. 7–8, pp. 714–720, 2005.

[4] A. V. Oppenheim and R. W. Schafer, *Discrete-Time Signal Processing***,** Prentice-Hall, 1999**.**

[5] S. Jayanti, Y. Kalyanaraman, N. Iyer, K. Ramani, "Developing an engineering shape benchmark for CAD models" in *Computer-Aided Design*, vol 38, no. 9, pp. 939–953, 2006.

[6] J. Ziv and A. Lempel, “A Universal Algorithm for Sequential Data Compression”, in *IEEE Transactions on Information Theory*, vol. 23, no. 3, pp. 337–343, 1977.

[7] D.A. Huffman: “A Method for the Construction of Minimum-Redundancy Codes”, in *Proceedings of the IRE*, vol. 40, no. 8, pp. 1098–1102, 1952.